Protein Science (1995), *4*:1346-1355. Cambridge University Press. Printed in the USA.

Simple models for the analysis of binding protein-dependent transport systems

BRIAN H. SHILTON[1] AND SHERRY L. MOWBRAY
Department of Molecular Biology, Swedish Agricultural University, Uppsala, Sweden

(RECEIVED October 26, 1994; ACCEPTED April 26, 1995)

Abstract

Mathematical modeling was used to evaluate experimental data for bacterial binding protein-dependent transport systems. Two simple models were considered in which ligand-free periplasmic binding protein interacts with the membrane-bound components of transport. In one, this interaction was viewed as a competition with the ligand-bound binding protein, whereas in the other, it was considered to be a consequence of the complexes formed during the transport process itself. Two sets of kinetic parameters were derived for each model that fit the available experimental results for the maltose system. By contrast, a model that omitted the interaction of ligand-free binding protein did not fit the experimental data. Some applications of the successful models for the interpretation of existing mutant data are illustrated, as well as the possibilities of using mutant data to test the original models and sets of kinetic parameters. Practical suggestions are given for further experimental design.

Keywords: bacterial transport; computer simulation; maltose transport; mutant proteins; periplasmic binding proteins

A large amount of experimental data is available for the binding protein-dependent transport systems of gram-negative bacteria (for reviews of these systems, see Ames, 1986; Boos & Lucht, 1995), but in the absence of an adequate theoretical framework that can be applied conveniently, it has often been hard to know how to evaluate it. As a result, key measurements have sometimes been lacking, and important conclusions missed or inadequately substantiated.

A schematic diagram of a generalized transport system (Fig. 1) illustrates the relevant molecular species and their minimal functional relationships. The modeling studies of Bohl and coworkers (Bohl et al., 1995; Bohl & Boos, 1995) have illustrated that some experimental results (e.g., Manson et al., 1985) cannot be explained using a model including only the simplest associations of the molecular components. On the other hand, a more complete model that allows for more possible interactions is too cumbersome for general use. The goal in the present paper is to determine the simplest models that can be used to explain the available data. Two such models will be elaborated, and suitable kinetic parameters derived using the experimental data for the *Escherichia coli* maltose transport system, primarily that described in Manson et al. (1985).

Reprint requests to: Sherry L. Mowbray, Box 590, Uppsala Biomedical Center, S-751 24 Uppsala, Sweden; e-mail: mowbray@xray.bmc.uu.se.

[1] Present address: Biotechnology Research Institute, 6100 Royalmount Avenue, Montreal, Quebec H4P 2R2, Canada.

Results

Models used

As a starting point, a generalized model of binding protein-dependent transport was constructed that describes the wild-type system as well as those in which the membrane components and/or the binding protein have functional mutations. This general scheme (Fig. 2) is far too complicated for mathematical modeling but does assist both in the design of simpler models, and as a reminder of their limitations. The framework was based on a number of considerations, including the following. (1) The transport of ligand through the outer membrane was not included, because of indications that this step is very fast ($10^9\ s^{-1}$; Wiegel, 1983). (2) Following Miller et al. (1983), the interaction of periplasmic binding protein (P) with the small molecule ligand (L) was modeled as a single step, although this is more likely to be a two-step process with ligand initially binding to an open form of P that subsequently closes, as illustrated in Figure 1 (see references cited in Mowbray, 1992, and Olah et al., 1993). (3) The binding protein has been considered to be a monomer (B.H. Shilton, unpubl. data) interacting with a single unit of the membrane transport complex (M), as is consistent with the experimental data of Hor and Shuman (1993). (4) Some data (Dean et al., 1992) suggest that at least two distinct forms of M exist in an equilibrium that is shifted toward M* in the normal case by the binding of the PL complex; some MalF and MalG mutants are able to transport ligand even without binding pro-

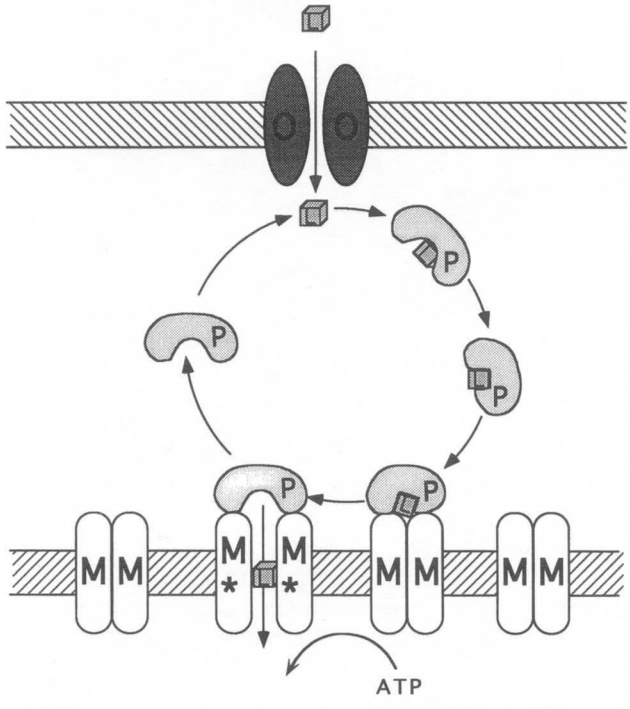

Fig. 1. Schematic view of the components of a binding protein-dependent transport system and the flow of ligand into the cell. Ligand (L) from the medium enters through the outer membrane, either by passive or facilitated diffusion (via a membrane porin, O). On reaching the periplasm, L can bind to an open form of a specific binding protein, P. P subsequently closes, giving rise to a species that is recognized by a complex of inner membrane transport proteins, M. This PLM complex carries out the transport of ligand across the inner membrane in a process requiring ATP. Empty P is then released into the periplasm, where it can bind ligand again and re-enter the transport cycle.

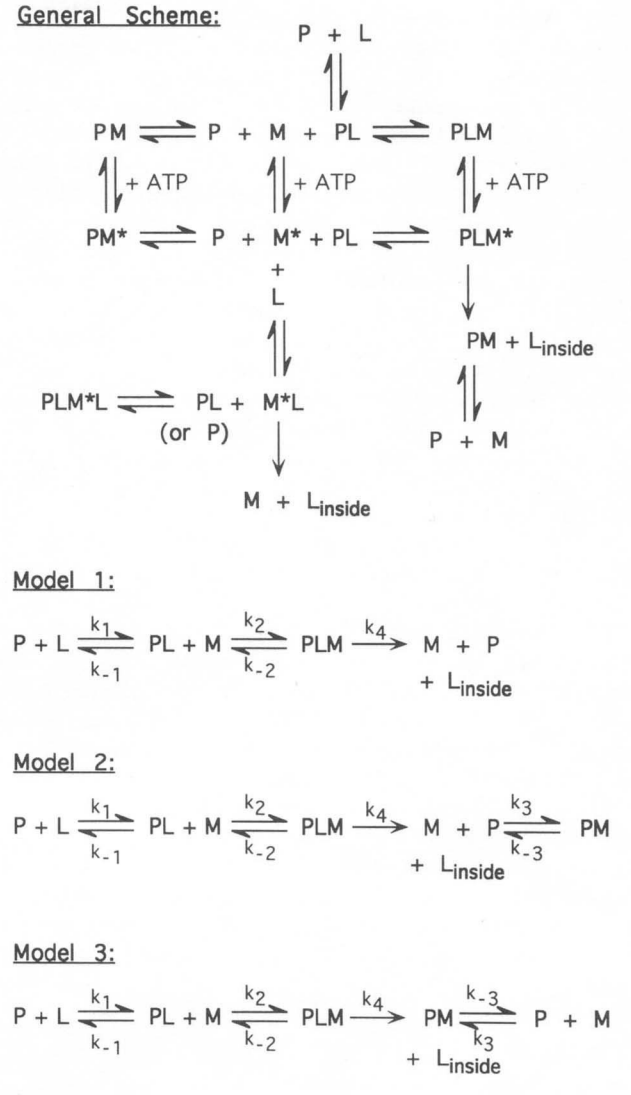

Fig. 2. Models for membrane transport analysis as described in the text. Components are identified as in Figure 1; complexes are indicated by strings of two or more letters.

tein (MBP-independent mutants) and presumably have changes in the normal equilibrium. These mutants also hydrolyze ATP in the absence of ligand (Davidson et al., 1992) supporting the contention that ATP is used for the activation (M to M*) step, not for ligand transport per se, and that this reaction is, in at least some cases, reversible. (5) Other experimental data have suggested that an interaction between unliganded binding protein and some form of the membrane transport complex might occur (Prossnitz et al., 1989; Davidson et al., 1992). For completeness, it should be considered that any form of M might have an affinity for P, PL, or L, but those already in complex with either PL or P are physically unlikely to bind a second P molecule, and wild-type M lacks appreciable affinity for free L (Shuman, 1982; Treptow & Shuman, 1985). (6) Only a single form of free P was considered, although both open and closed forms are expected to exist in solution (Jacobson et al., 1991; Flocco & Mowbray, 1994; Wolf et al., 1994).

Models 1–3 (Fig. 2) were intended to describe the events outlined in the general scheme in the simplest pathways possible. All ignore any M/M* equilibrium without some form of P bound, which should be well toward M in the case of wild-type membrane transport complex, and which will be nonproductive in the usual situation. In addition, they combine two physical steps into k_4, and assume that dissociation of PLM* into PL and M* is disfavored. The step involving the hydrolysis of ATP has generally been assumed to be irreversible and rate limiting, but this has not been proven explicitly and indeed is demonstrated below to be indeterminate with the presently available data. Model 1 considers only the simplest interactions of P with L, and PL with M, whereas Models 2 and 3 include as well an interaction between P and M. Both of the latter describe interactions of P with any form of M (e.g., M or M*) as PM complexes only. In Model 2, the interaction of P with M is viewed purely as a competition with the ligand-bound binding protein, whereas in Model 3, it is viewed as a consequence of the transport process itself. Models 1 and 2 are identical to those considered by Bohl and coworkers (Bohl et al., 1995; Bohl & Boos, 1995).

Derivation of relevant expressions

Using a treatment similar to that described previously (Bohl et al., 1995; Bohl & Boos, 1995), the mathematical relationships

describing the reaction velocity and K_m's were derived. Briefly, a system of simultaneous equations was set up, each representing the steady-state achieved for a particular reaction component during measurements of the rate of transport. (A steady state was assumed because transport rates remain constant for one or more minutes in the usual assays; it was also assumed that the ligand concentration in the periplasm is constant and equal to that in the medium.) Solution of these relationships, in conjunction with mass balance equations for the two proteins, gave rise to expressions for [PLM] in terms of the kinetic constants (k_1, k_{-1}, k_2, k_{-2}, k_3, k_{-3}, and k_4) and concentrations of total protein ($[M]_{tot}$ and $[P]_{tot}$) and free ligand ([L]) (see Supplementary material in the Electronic Appendix).

The velocity of transport (v) is defined as the rate at which L crosses the membrane at the k_4 step and is equal to k_4[PLM]. In all three models, this rate reaches a maximum (V_{max}) at $k_4[PLM]_{max} = k_{cat}[M]_{tot}$. In Models 1 and 2, $[PLM]_{max} = [M]_{tot}$ and the catalytic constant $k_{cat} = k_4$. In Model 3, $[PLM]_{max}$ is less than $[M]_{tot}$, equaling $[k_{-3}/(k_{-3} + k_4)][M]_{tot}$, and so $k_{cat} = (k_{-3}k_4)/(k_{-3} + k_4)$. Both k_{-3} and k_4 will therefore be greater than k_{cat} in that model.

$K_{m\{L\}}$ was then derived by finding [L] (as a function of $[P]_{tot}$) at half the maximum velocity. Similarly, $K_{m\{Ptot\}}$ represents the $[P]_{tot}$ that would give rise to a velocity half the maximum possible for any given [L]; $[P]_{tot}$ was used instead of the conventional free P concentration, because only the former is an experimentally measurable quantity.

The general expressions for velocity and the two K_m's are not shown here because they are extremely large, although the system is easily manipulated with the program Mathematica (see Supplementary material in the Electronic Appendix). Expressions for two useful limiting cases, $K_{m\{L\}}$ at infinitely high $[P]_{tot}$ (defined as $K_{m\{L\text{-}iP\}}$) and $K_{m\{Ptot\}}$ at infinitely high [L] ($K_{m\{P\text{-}iL\}}$), are:

Model 1

$$K_{m\{L\text{-}iP\}} = 0 \tag{1}$$

$$K_{m\{P\text{-}iL\}} = \frac{[M]_{tot}}{2} + \frac{k_{-2} + k_4}{k_2} \tag{2A}$$

$$= \frac{[M]_{tot}}{2} + K_{d\{PL\}}(1 + k_4/k_{-2}) \tag{2B}$$

Model 2

$$K_{m\{L\text{-}iP\}} = \frac{k_{-1}k_3(k_{-2} + k_4)}{k_1k_2k_{-3}} \tag{3A}$$

$$= \frac{K_{d\{L\}}K_{d\{PL\}}(1 + k_4/k_{-2})}{K_{d\{P\}}} \tag{3B}$$

$$K_{m\{P\text{-}iL\}} = \frac{[M]_{tot}}{2} + \frac{k_{-2} + k_4}{k_2} \tag{4A}$$

$$= \frac{[M]_{tot}}{2} + K_{d\{PL\}}(1 + k_4/k_{-2}) \tag{4B}$$

Model 3

$$K_{m\{L\text{-}iP\}} = \frac{k_{-1}k_3(k_{-2} + k_4)}{k_1k_2(k_{-3} + k_4)} \tag{5A}$$

$$= \frac{K_{d\{L\}}K_{d\{PL\}}(1 + k_4/k_{-2})}{K_{d\{P\}}(1 + k_4/k_{-3})} \tag{5B}$$

$$K_{m\{P\text{-}iL\}} = \frac{[M]_{tot}}{2} + \frac{k_{-3}(k_{-2} + k_4)}{k_2(k_{-3} + k_4)} \tag{6A}$$

$$= \frac{[M]_{tot}}{2} + K_{d\{PL\}}\frac{(1 + k_4/k_{-2})}{(1 + k_4/k_{-3})} \tag{6B}$$

$$= \frac{[M]_{tot}}{2} + \frac{k_{cat}(k_{-2} + k_4)}{k_2k_4}, \tag{6C}$$

where the dissociation constants for various interactions are: $K_{d\{L\}} = k_{-1}/k_1$, $K_{d\{PL\}} = k_{-2}/k_2$, and $K_{d\{P\}} = k_{-3}/k_3$. Note that Equations 3 and 5 approach zero as $K_{d\{P\}}$ becomes large, that is, as the affinity between the membrane complex and the unliganded binding protein decreases, Models 2 and 3 both become more similar to Model 1.

In both Models 2 and 3, substitution of $K_{m\{L\text{-}iP\}}$ into the $K_{m\{P\text{-}iL\}}$ equation gives:

$$K_{m\{P\text{-}iL\}} = \frac{[M]_{tot}}{2} + \frac{K_{d\{P\}}K_{m\{L\text{-}iP\}}}{K_{d\{L\}}} \tag{7}$$

and by rearrangement:

$$\frac{K_{d\{P\}}}{K_{d\{L\}}} = \frac{k_1k_{-3}}{k_{-1}k_3} = \frac{(K_{m\{P\text{-}iL\}} - [M]_{tot}/2)}{K_{m\{L\text{-}iP\}}}, \tag{8}$$

which gives a value for $k_1k_{-3}/k_{-1}k_3$, if $K_{m\{P\text{-}iL\}}$, $K_{m\{L\text{-}iP\}}$, and $[M]_{tot}$ are known, and defines $[M]_{tot}/2$ as a minimum for $K_{m\{P\text{-}iL\}}$ (because $K_{d\{P\}}/K_{d\{L\}}$ cannot be negative).

Rearrangement of the $K_{m\{P\text{-}iL\}}$ equations gives:

$$K_{m\{P\text{-}iL\}} - \frac{[M]_{tot}}{2} = \frac{(k_{-2} + k_4)}{k_2} \tag{9}$$

in Models 1 and 2 (from Equations 2A and 4A), and

$$K_{m\{P\text{-}iL\}} - \frac{[M]_{tot}}{2} = \frac{k_{cat}(k_{-2} + k_4)}{k_2k_4} \tag{10}$$

in Model 3 (from Equation 6C). Where $K_{m\{P\text{-}iL\}}$, $[M]_{tot}$, and k_4 (or k_{cat}) are known, Equations 9 and 10 can be used to give lower limits for the value of k_2 (because k_{-2} must be ≥ 0).

Estimation of kinetic parameters from data for the wild-type maltose system

The catalytic constant, k_{cat}

The value used for k_{cat} in the present work (230 s^{-1}) is based on the largest rates of transport in cells (2–2.4 nmol/min/10^8 cells; Szmelcman et al., 1976; Manson et al., 1985), and the

greatest expected number of membrane transport complexes (M) per cell (100–1,000; Shuman, 1982). Because it is a first-order rate constant related to the membrane transport complexes, it is dependent on their number, not on their concentration. If there are larger or smaller amounts of membrane transport complex, a smaller or larger k_{cat} would be required, and other parameters would need to be adjusted to fit the experimental data. It should also be pointed out that, because this parameter represents several discrete physical steps, including that involving hydrolysis of ATP, it may well vary with the energy state of the cell, as is consistent with the experimental data of Kehres and Hogg (1992).

Absolute velocity

A maximum absolute velocity in normal cells can be calculated using the measured rate of transport and estimates for the volume of the periplasm. Assuming that *E. coli* is 1 μm in diameter and 2 μm long, its surface area is approximately 8×10^6 nm^2. If the periplasm is on average 7.5 nm wide, this would give the volume of the periplasm of a single cell as 6×10^{-17} L. If there is a maximum of 2.4 nmol maltose transported by 10^8 cells per minute, a rate of 0.0067 M s^{-1} is obtained as an approximation for the absolute V_{max} of transport. This value might, however, be lower if alternate values of the periplasmic dimensions (Oliver, 1987; van Wielink & Duine, 1990) are used. It might also be higher if the entire volume of the periplasm is not available, as for example if the transport systems are clustered at the poles of the cells as is suggested by the data of Maddock and Shapiro (1993). In these cases other "known" quantities would need to be adjusted in proportion, and the parameters derived would differ somewhat, as illustrated below.

Total protein concentrations

Maltose-binding protein (MBP) has been estimated to be present in normal cells after induction at a level of 30,000 molecules per cell (Shuman, 1982). If the available periplasmic volume is 6×10^{-17} L, $[MBP]_{tot}$ (i.e., $[P]_{tot}$) would be maximally 1 mM. If there are 1,000 membrane transport complexes, this would give a value for $[M]_{tot}$ of 35 μM. Although the concentration of a membrane protein is in reality a two-dimensional property, the inner membrane complex is treated for the present purposes as a "three-dimensional" protein that does not diffuse.

Diffusion limit for k_2

Simple diffusion calculations suggest a maximum for the expected rate of collision of MBP with the inner membrane complex, i.e., k_2. Assuming that only MBP (and not the membrane complex) is diffusing, and using the Arrhenius equation:

$$\text{rate} = 4\pi(r_e)D_P N_0/1{,}000,$$

where r_e is the encounter distance (estimated to be 5 nm, roughly twice the radius of gyration of MBP), D_P is the diffusion constant for MBP in the periplasm (3×10^{-10} cm^2/s; Brass et al., 1986), and N_0 is Avogadro's number, a value of 1.1×10^6 M^{-1} s^{-1} is obtained.

Michaelis constant for maltose

The values of $K_{m\{mal\}}$ (i.e., $K_{m\{L\}}$ for this case) at $[MBP]_{tot}$ up to the normal induced level have been reported for whole cells by Manson et al. (1985) and are shown in the plot in Figure 3A. It was determined empirically that the data give an excellent nonlinear fit to an equation of the form: $y = a/x + b$ (in this case, $K_{m\{mal\}} = 7.41839 \times 10^{-7} + (2.04909 \times 10^{-11})/[MBP]_{tot}$), indicating that $K_{m\{mal\text{-}i MBP\}}$ (i.e., $K_{m\{L\text{-}i P\}}$ for this case) is approximately 0.74 μM.

Dissociation constant for maltose

The dissociation constant for binding of maltose to MBP, $K_{d\{mal\}}$ (i.e., $K_{d\{L\}}$), is equal to k_{-1}/k_1, and has been measured as 1–4 μM (Schwartz et al., 1976; Szmelcman et al., 1976; Richarme & Kepes, 1983), a value that is in good agreement with individual estimates of k_1 (2.3×10^7 M^{-1} s^{-1}) and k_{-1} (90 s^{-1}) from fluorescence spectroscopy (Miller et al., 1983).

Michaelis constant for MBP

The estimation of $K_{m\{MBP_{tot}\}}$ (i.e., $K_{m\{P_{tot}\}}$) is somewhat problematic, because previous studies have apparently not taken into account either the fact that this quantity will be dependent on [mal] or that a double reciprocal analysis of $1/v$ versus 1/[MBP] at any given ligand concentration yields a nonlinear plot. Despite these problems, the values of $K_{m\{MBP_{tot}\}}$ reported to date are comfortingly close to each other – 90 μM in vivo with

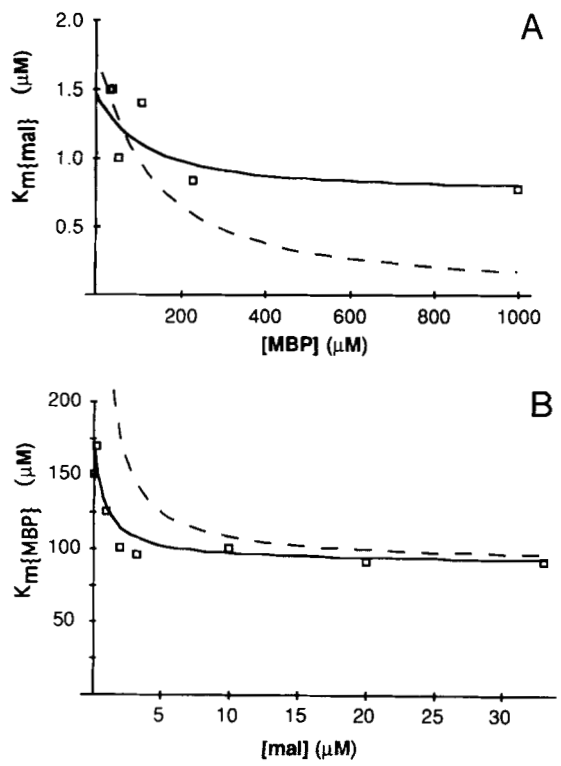

Fig. 3. Agreement of the predicted curves for Model 1 (dashed lines) and Model 2 (solid lines), with the experimental data. Values used for Model 1 were: $k_1 = 1.8 \times 10^8$ M^{-1} s^{-1}; $k_{-1} = 360$ s^{-1}; $k_2 = 4 \times 10^6$ M^{-1} s^{-1}; $k_{-2} = 64$ s^{-1}; $k_4 = 230$ s^{-1} and those for Model 2 were from case 1 in Table 1. **A:** $K_{m\{mal\}}$ at various $[MBP]_{tot}$; experimental data reported by Manson et al. (1985) are shown as open squares. **B:** $K_{m\{MBP_{tot}\}}$ at various [mal]; experimental data were extracted from Manson et al. (1985) as described in the text and are shown as open squares.

33 μM maltose (Manson et al., 1985) and 25–50 μM in an in vitro vesicle system with 10 μM maltose (Dean et al., 1992).

In practice, the $K_{m\{P_{tot}\}}$ at a given ligand concentration can be estimated from a v versus $[P]_{tot}$ plot by finding $[P]_{tot}$ that gives rise to half the maximum velocity for that [L] (the maximum occurring at infinite $[P]_{tot}$). These maximum velocities were therefore estimated as carefully as possible from the nonlinear $1/v$ versus 1/[MBP] plots for the data extracted from Manson et al. (1985), and checked for consistency by graphing them versus 1/[mal] (a plot that should be linear according to both Models 2 and 3, with a slope of $K_{m\{L\text{-}iP\}}/V_{max}$ and an intercept of $1/V_{max}$). The estimate for $K_{m\{mal\text{-}iMBP\}}$ obtained in this way (0.7 μM) is in good agreement with that obtained above from the empirical fit of the $K_{m\{mal\}}$ data. Knowing the maximum velocity at any given concentration of maltose, it is then possible to determine the concentration of MBP that gives rise to half that rate of transport. The resulting $K_{m\{MBP_{tot}\}}$ estimates at different concentrations of maltose are plotted in Figure 3B. A good empirical fit of these points to $K_{m\{MBP_{tot}\}} = 0.000090961 + (2.6582 \times 10^{-11})/[mal]$ suggests that $K_{m\{MBP\text{-}imal\}}$ (i.e., $K_{m\{P\text{-}iL\}}$ for this case) is approximately 91 μM.

Fitting additional parameters in the models

Model 1

Neither the $K_{m\{mal\}}$ nor the $K_{m\{MBP_{tot}\}}$ data could be fitted using this model; the type of behavior found is illustrated in Figure 3. In Figure 3A, adequate agreement is seen for $K_{m\{mal\}}$ at the lower concentrations of binding protein, but gross disagreement at the highest level. Because the latter represents the normal wild-type situation for which most data exist, its failure must be considered a fatal flaw in the model. Even with strains that overproduce wild-type binding protein many-fold, the $K_{m\{MBP\text{-}imal\}}$ has not been observed to decrease substantially in the manner predicted by Model 1 (H. Shuman, unpubl. data). In Figure 3B, the behavior of $K_{m\{MBP_{tot}\}}$ is seen to deviate most strongly at lower concentrations of maltose. The parameter set in this illustration was chosen to minimize the discrepancies in the two plots and so must be considered a best-case scenario.

Model 2

A situation where the entire periplasm is available to both P and M was considered (case 1) as well as one where both binding protein and membrane transport complex are concentrated fivefold at the poles of the cell (case 2). The expected absolute velocities and $K_{m\{MBP_{tot}\}}$ will be greater by a factor of five in the latter case.

The estimate for k_{cat} gives a value for k_4 in this model. Equation 8 dictates a value of $k_1k_{-3}/k_{-1}k_3$ of 99 in case 1 and 497 in case 2, allowing k_{-3} to be expressed in terms of k_1, k_{-1}, and k_3. A lower limit for k_2 of 3.2×10^6 M^{-1} s^{-1} for case 1 and 6.3×10^5 M^{-1} s^{-1} in case 2 can be obtained from Equation 9, by setting $k_{-2} = 0$ and rearranging. (If k_4 is larger than 230 s^{-1}, e.g., because fewer molecules of membrane complex are present, k_2 would need to be even larger.) With this same information, an expression for k_{-2} in terms of k_2 and k_4 can be derived. Somewhat simpler formulae can then be obtained by substituting these relationships into the general expressions for $K_{m\{mal\}}$ and $K_{m\{MBP_{tot}\}}$.

Any combination of k_2 and k_{-2} values that fulfills Equation 9 works in identical fashion in the system; $K_{d\{MBP\text{-}mal\}}$ ($K_{d\{PL\}} = k_{-2}/k_2$) is therefore not completely determined. In both cases given, a pair was chosen that gave a k_2 value just above the minimum allowed (because it is already at or near the diffusion limit); the resulting k_{-2} values were roughly 20 s^{-1} and were arbitrarily set to that value to simplify comparison. Even small increases in the k_2 values require quite large increases in k_{-2} for the necessary relationships to hold. Because only the ratio of k_3 to k_{-3} and not their absolute magnitude is important, k_3 was arbitrarily set to be equal to k_2. When these substitutions are made into the more general expression for $K_{m\{mal\}}$, only k_1, k_{-1}, and $[MBP]_{tot}$ remain. If the further assumption is made that $K_{d\{mal\}}$ is 1 μM, i.e., that $k_{-1} = k_1 \times 10^{-6}$ M, a value of 1.8×10^8 M^{-1} s^{-1} is required for k_1 and 180 s^{-1} for k_{-1} to match the experimental $K_{m\{mal\}}$'s. $K_{d\{mal\}}$'s even as high as 3 μM are not allowed without k_1 and k_{-1} substantially larger than the experimentally determined values (Miller et al., 1983).

Model 3

Only the situation where the entire periplasm is available to both P and M is considered here.

A lower limit of 3.2×10^6 M^{-1} s^{-1} is obtained for k_2 from Equation 10, by setting $k_{-2} = 0$ and rearranging. As in Model 2, the value of k_{-2} is related to that used for k_2, and so $K_{d\{MBP\text{-}mal\}}$ is not determinate.

The catalytic constant, k_{cat}, is in this case $(k_{-3}k_4)/(k_{-3} + k_4)$. Because k_{cat} is assumed to be 230 s^{-1}, and both k_4 and k_{-3} must be positive real numbers, each must be at least 230 s^{-1}. Equation 8 dictates a value for $(k_1k_{-3})/(k_{-1}k_3)$ of 100, allowing k_{-3} to be expressed in terms of k_1, k_{-1}, and k_3 as before. Combined with the knowledge that k_{-1}/k_1 is on the order of 1 μM, these expressions dictate that k_3 must be at least 2.35×10^6 M^{-1} s^{-1}. As it seems physically unlikely that k_3 will be greater than k_2, the former constant is most probably in the range of 2.35×10^6 to 3.4×10^6 M^{-1} s^{-1} (the latter value based on analogy to Model 2 and remembering the estimated diffusion limit); these two limits were used to elaborate cases 1 and 2. Again, simpler formulae were obtained by substituting the known relationships into the general expressions for $K_{m\{L\}}$ and $K_{m\{P_{tot}\}}$. Because it is known that k_{-1} is approximately equal to $k_1 \times 10^{-6}$ M, the experimental values of $K_{m\{MBP_{tot}\}}$ determine that k_1 is on the order of 2×10^8 M^{-1} s^{-1}. As for Model 2, larger values for $K_{d\{mal\}}$ are not allowed. As case 2 illustrates, smaller values of k_3 rapidly dictate values of k_4 that seem rather large for a chemical step (the average enzyme operates at a rate of around 20 s^{-1}; Walsh, 1979). In addition, the ratio of $K_{d\{MBP\}}$ to $K_{d\{MBP\text{-}mal\}}$ suggests that this parameter set is less likely, because the liganded binding protein would be expected to have a higher affinity.

Trial parameter sets

The four sets of parameters obtained from these analyses are shown in Table 1. The agreement of the model curves with the experimental data is illustrated for Model 2 (case 1) in Figure 3A and B; the fit to the other parameter sets is essentially identical. The predicted absolute velocity for 1 mM concentrations of MBP and 33 μM maltose (the maximum concentrations used by Manson et al., 1985) are 0.0073 M s^{-1} for all except Model 2, case 2, where it is 0.0365 M s^{-1}, in good agreement with the ex-

Table 1. *Parameter sets giving good fits to the experimental data for the maltose transport system in Models 2 and 3, derived as explained in the text*

Parameter	Model 2, case 1	Model 2, case 2	Model 3, case 1	Model 3, case 2
k_1 (M^{-1} s^{-1})	1.8×10^8	1.8×10^8	2×10^8	2×10^8
k_{-1} (s^{-1})	180	180	200	200
k_2 (M^{-1} s^{-1})	3.4×10^6	6.8×10^5	3.4×10^6	3.4×10^6
k_{-2} (s^{-1})	20	20	62.4	1361
k_3 (M^{-1} s^{-1})	3.4×10^6	6.8×10^5	3.4×10^6	2.35×10^6
k_{-3} (s^{-1})	338	338	338	233
k_4 (s^{-1})	230	230	721	15,733
$[M]_{tot}$ (μM)	35	175	35	35
$[P]_{tot}$ (μM)	1,000	5,000	1,000	1,000
$K_{d\{mal\}} = k_{-1}/k_1$ (μM)	1	1	1	1
$K_{d\{MBP\text{-}mal\}} = k_{-2}/k_2$ (μM)	5.9	29	18	400
$K_{d\{MBP\}} = k_{-3}/k_3$ (μM)	99	497	99	99
$K_{d\{MBP\}}/K_{d\{MBP\text{-}mal\}}$	16.9	17.1	5.4	0.25

perimental values. Note that the rate-limiting step cannot be determined with the available experimental data: in Model 2, k_4 (the ATP-consuming step) is rate-limiting, whereas in Model 3, it is k_{-3} (the dissociation of the PM complex).

Evaluation of mutant results

Functional mutations can affect the binding of transport components, the efficiency with which they work together, or both. Given the experimental behavior of mutants, it is possible to utilize Models 2 and 3 to suggest which properties are most likely to be affected, as well as to test the models and parameter sets that have been derived. It should be stated that the simple models may not be appropriate for use with mutants of the membrane components that disturb the binding protein-independent $M \leftrightarrow M^*$ equilibrium (as is likely to be the case in MBP-independent mutants) but ought to be useful for other types of mutations of either binding protein or membrane components.

The parameters k_1 and k_{-1} determine the affinity of binding protein for ligand, with $K_{d\{L\}} = k_{-1}/k_1$. Equations 3B and 5B illustrate that in Models 2 and 3, effects on $K_{d\{L\}}$ have directly proportional effects on $K_{m\{L\text{-}iP\}}$; this statement is true in the general case of $K_{m\{L\}}$, as well. Thus, if both $K_{m\{L\}}$ and $K_{d\{L\}}$ are measured, it is possible to correct the $K_{m\{L\}}$ values for k_1 or k_{-1} effects, allowing changes in other kinetic constants to be seen more clearly. That is:

$$K_{m\{L\text{-}iP\}\text{-mut}}\text{-corrected} = K_{m\{L\text{-}iP\}\text{-mut}} * \frac{K_{d\{L\}\text{-wt}}}{K_{d\{L\}\text{-mut}}}, \qquad (11)$$

where the "mut" and "wt" suffixes refer to the mutant and wild-type properties, respectively.

Changes in the affinity of ligand-bound binding protein for the membrane transport complex ($K_{d\{PL\}}$) through mutations in any of the proteins are expressed as effects in k_2 and/or k_{-2}. It is likely to be a common feature of these mutations that k_3 and/or k_{-3} will also be affected. Some mutations might of course affect $K_{d\{P\}}$ alone.

Decreases in the efficiency with which the membrane transport complex and the binding protein work in concert will be reflected in decreased values for k_4. Somewhat counterintuitively, decreases in k_4 are predicted to result in decreases in both $K_{m\{L\}}$ and $K_{m\{P_{tot}\}}$ in all of the parameter sets presented here except Model 3, case 2.

If the kinetic parameters for any given mutant and wild-type system were known, it would be simple to use the two models to predict the changes in experimental results for that mutant. In practice, changes in the experimental behavior will be observed without initially knowing what changes in kinetic parameters they reflect. The most productive approach then will be that of looking for characteristic relationships between experimentally measurable quantities as a means of establishing which kinetic parameters are affected. The most useful plot for a preliminary analysis is V_{max} versus $K_{m\{L\}}$, because these quantities are both obtainable in vivo. The formulae for $K_{m\{L\text{-}iP\}}$ in Equations 3 and 5 can be used cautiously for this purpose, a procedure that is likely to be safest for mutants with overproduced binding proteins. (It should be remembered both that the $K_{m\{P_{tot}\}}$ may be dramatically increased, and that mutation may result in less protein being produced, either of which might invalidate the assumption of saturation; the latter should, of course, be checked by gel electrophoresis.) The predicted behavior of maltose transport system mutants where different kinetic parameters are altered is illustrated in Figure 4A–F. Both for ease of comparison and because the absolute magnitude of transport velocity is not really known in vivo (as discussed above), the V_{max} values have been normalized to those of the wild type. Although $K_{m\{P_{tot}\}}$ is not easily measured in vivo, the results of the V_{max} versus $K_{m\{L\}}$ plots can be checked with the formulae for $K_{m\{P\text{-}iL\}}$ to ensure that the assumption of infinite $[P]_{tot}$ has not been substantially violated.

Alteration of different kinetic parameters gives rise to distinct patterns of effects. This provides the potential to determine the nature of particular mutations and to suggest the model and parameter set likely to be appropriate for the system as a whole. That these goals are feasible for real mutations is illustrated by the experimental data for the related ribose transport system in

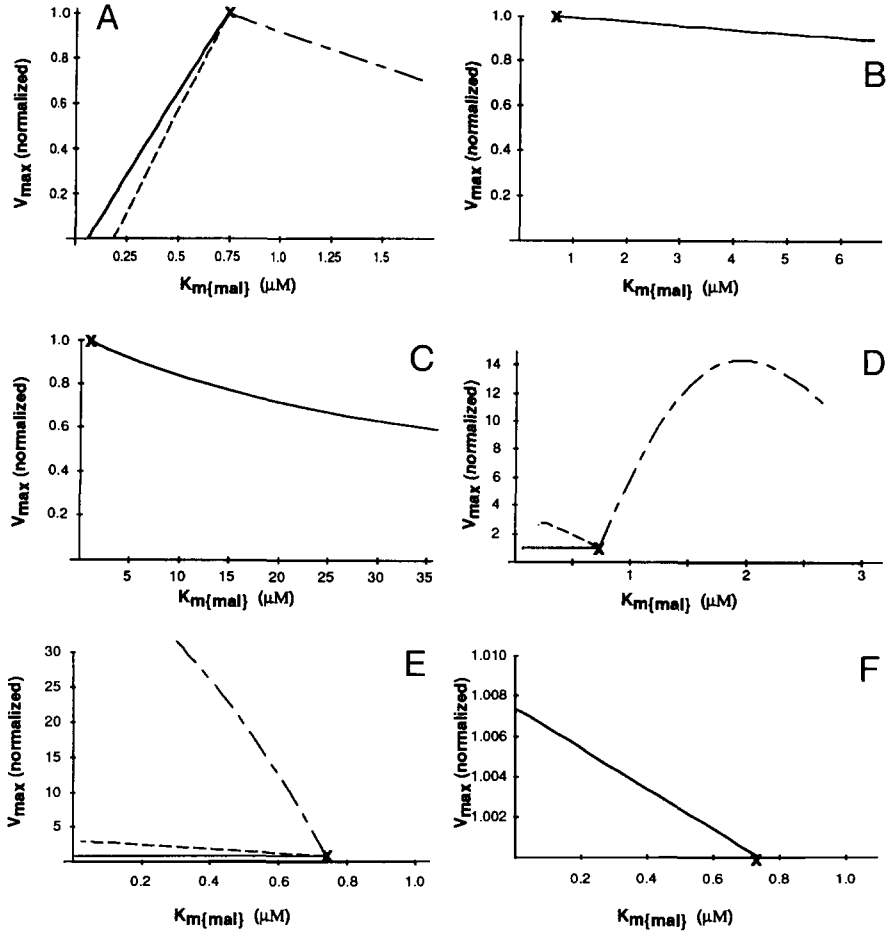

Fig. 4. Predicted relationships between V_{max} and $K_{m\{L\text{-}iP\}}$ in various classes of mutations in the transport proteins. To mimic the effects of mutations, one or more kinetic constants was altered from those given in Table 1, and the resulting V_{max} and $K_{m\{L\text{-}iP\}}$ were calculated using Models 2 and 3. Kinetic constants were altered over a range of 100-fold in each case. **A:** Decrease in k_4. **B:** Increase in k_{-2}. **C:** Decrease in k_2. **D:** Proportional increases in both k_{-2} and k_{-3}. **E:** Increase in k_{-3}. **F:** Decrease in k_3. Velocities have been normalized such that the wild-type velocity is 1.0, and the behavior of the wild-type system is marked in each plot as "X." Curves for Model 2 are shown as solid lines; those for Model 3, case 1, as dashed lines (– – –), and case 2 as broken lines (—— –). All plots for the two cases of Model 2 coincide exactly and so only a single curve is shown for that model; curves for all cases coincide for B, C, and F.

Figure 5. Figure 5A shows a plot of the V_{max} and $K_{m\{rib\}}$ measurements obtained with various mutants of the ribose-binding protein (drawn from Binnie et al., 1992). After correction for $K_{d\{rib\}}$ (that is, k_1 or k_{-1}) effects using Equation 11 (Fig. 5B), the data for most of the mutants show the characteristic pattern of k_4 changes illustrated in Figure 4A (all cases but Model 3, case 2). (A large amount of scatter in the plot is not surprising given the combined errors of three experimental measurements.) A similar pattern of apparent k_4 effects has also been observed for the arabinose transport system (Kehres, 1992), but without accompanying changes in $K_{d\{ara\}}$. Two "outliers" in Figure 5B show different types of changes. One shows a decreased $K_{m\{rib\}}$-corrected with little difference in V_{max}, consistent with a mutation affecting $K_{d\{P\}}$ (that is, k_3 or k_{-3}; either Model 2 or Model 3, case 1, in Fig. 4D, E, or F). The site of this mutation (I111R) is on the surface of the protein, but outside the actual region involved in transport interactions, based on the location of other mutations affecting transport; it is also distant from the sugar-binding site. Effects on $K_{d\{P\}}$ would, however, agree with the observation that mutation of this residue causes an increase in $K_{d\{rib\}}$ (i.e., weaker binding) and had been speculated to do so by stabilizing an open form of the binding protein (assuming that it is the closed form that competes for M). A second outlier with greatly decreased V_{max} but little change in $K_{m\{rib\}}$-corrected is most likely the result of an altered k_4 together with some other difference, probably one affecting $K_{d\{PL\}}$ (compare with Fig. 4A,B,C). The site of this mutation (G134A) is also somewhat special, in that X-ray structural studies (Björkman et al., 1994) have implicated it as a location at which the main chain of the binding protein is likely to be involved in interactions with the membrane transport complex. The availability of the equivalent type of data for the maltose system would allow a similar analysis for mutants in that system.

More sophisticated experiments can be carried out in an in vitro vesicle system (Dean et al., 1989), which would allow better control of the protein and ligand concentrations, and therefore routine measurement of $K_{m\{MBP_{tot}\}}$ as well as $K_{m\{mal\}}$. However, the basic behavior of that system will need to be established more firmly; although the $K_{m\{MBP_{tot}\}}$ (Dean et al., 1992) is indeed similar to that measured in cells, more data are needed (e.g., $K_{m\{mal\}}$ experiments) to be certain whether this is really due to similar kinetic constants or merely coincidental.

Discussion

The present study was begun soon after we initiated X-ray structural work on a mutant of the maltose-binding protein. It was realized almost immediately that, even with known structures of many mutants, it would be very difficult to explain their phenotypes in the absence of accessible models for maltose transport. The resulting models have given us a much broader understanding of the ways in which physical events may be man-

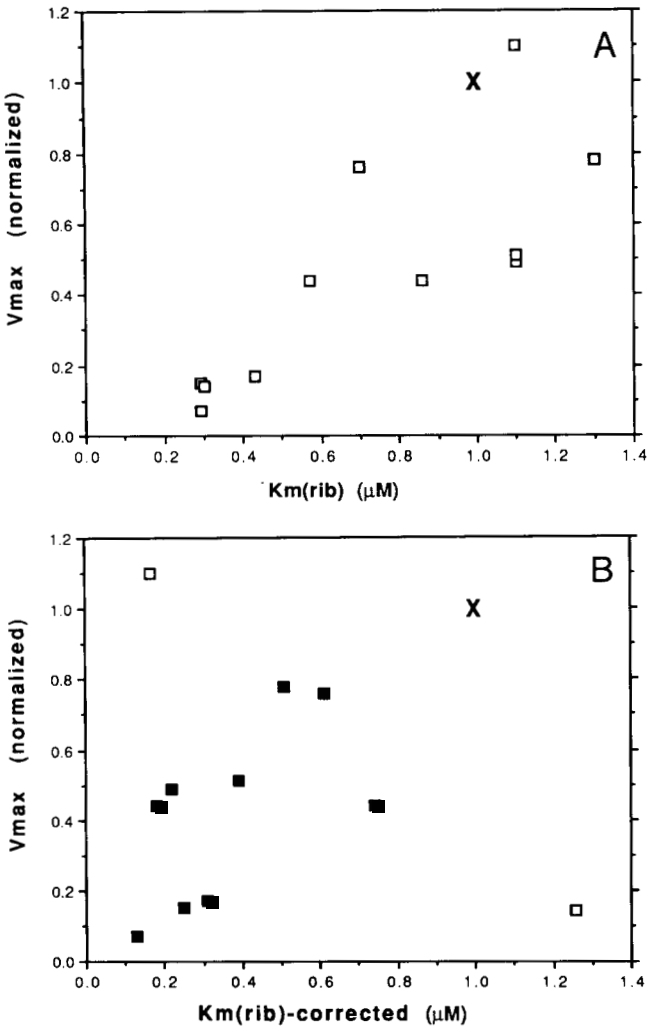

Fig. 5. Behavior of the ribose transport system with mutations in the binding protein, calculated from data presented in Binnie et al. (1992). **A:** V_{max} of transport versus $K_{m\{rib\}}$; both values have been normalized to that of the wild type. **B:** The same data where each $K_{m\{rib\}}$ has been corrected for changes in $K_{d\{rib\}}$ using Equation 11. In the latter plot, mutants that seem to show a predominant k_4 effect are shown as filled squares, and two others as open squares. Wild-type result is shown as "X" in both plots.

ifested in the behavior of the experimental system. These studies provide further support for suggestions that both ligand-free and ligand-bound forms of binding protein can interact with the membrane transport complex (Prossnitz et al., 1989; Davidson et al., 1992; Bohl et al., 1995; Bohl & Boos, 1995; Boos & Lucht, 1995). This competition has important consequences for the behavior of the system, allowing it to remain responsive to changes in ligand concentrations over a wide range of binding protein concentrations (a critical feature in a system where the binding protein is inducible and therefore present at fluctuating levels). In Model 2, the ligand-free protein is effectively a competitive inhibitor, and in Model 3 the interaction also has aspects of product inhibition. The observation of Davidson et al. (1992) that the addition of MBP in the absence of maltose results in a rate of ATP hydrolysis roughly 1/10 that found in the case where both MBP and maltose are added to the wild-type membrane transport complex argues that a competitive interaction like that described in Model 2 does occur and agrees with the ratio of liganded and unliganded MBP affinities suggested by that model. On the other hand, the scenario described by Model 3 must exist, by virtue of the transport mechanism itself; it is not clear, however, that it will be a kinetically distinguishable step. Furthermore, the present data do not allow a decision about which parameter set for either model might be most useful for the maltose system, although Model 3, case 2, appears less likely than the other parameter sets. Additional experimental data are obviously required to determine which model will be most appropriate, and indeed whether or not some localization of the transport proteins in the periplasm is an important feature.

Both of the simple models provide a good explanation for the in vivo data of the wild-type maltose transport system. However, what applies to the whole cell may not be satisfactory for the vesicle system; better measurements of protein quantities/concentrations and other values are clearly desirable for further characterization of both systems. It is worth a reminder in this context that $K_{m\{L\}}$ (the concentration of L that gives rise to half-maximal transport) is not the same as $K_{d\{L\}}$ (the dissociation constant), and $K_{m\{Ptot\}}$ is not the same as $K_{d\{Ptot\}}$, that is, activity does not necessarily reflect affinity. Careful measurements of all of these quantities are needed for the results to be meaningful. In addition, the use of "standard" concentrations of either ligand or binding protein for comparison of the effects of different mutations is fraught with danger in a situation where both $K_{m\{L\}}$ and $K_{m\{Ptot\}}$ may change with mutations, and in ways that are not intuitively obvious.

The k_1 and k_{-1} required to fit the transport data in any model are similar to the values measured in solution (Miller et al., 1983) and are in good agreement with the measured $K_{d\{mal\}}$ (Schwartz et al., 1976; Szmelcman et al., 1976; Richarme & Kepes, 1983). The value of k_2 in all cases is required to be as large as that predicted from simple calculations based on the measured diffusion of MBP in the periplasm (which consider collision only). The fact that these estimates are so similar suggests that some means of speeding up this association, such as two-dimensional diffusion along the membrane, is not necessary. The fact that a true upper limit for k_2 cannot yet be determined unfortunately means that a wide range of values are possible for $K_{d\{PL\}}$. In vitro studies seem to offer the best hope of resolving this ambiguity.

It is ironic that, because $K_{d\{P\}}$ can be determined in the models in the present study, whereas $K_{d\{PL\}}$ cannot, the relative strength of these two interactions is not known (see Table 1). It is also not clear whether it is an open or a closed form of ligand-free binding protein (such as those observed for the related glucose/galactose- and histidine-binding proteins; Flocco & Mowbray, 1994; Wolf et al., 1994) that is competing. Although small angle X-ray scattering studies show that the closed form is rare in the absence of ligand (B.H. Shilton, unpubl. data), it seems more likely to compete effectively with the closed ligand-bound form. Alternatively, the interaction of the ligand-free protein may be based on a single domain of MBP and so be independent of the open or closed state. It should also be noted that in the present formulation of the models, k_3 and k_{-3} reflect the *apparent* affinity of the *total* population of the unliganded MBP and make no reference to any subpopulations

with differing affinities. If only a single species of ligand-free binding protein interacts appreciably (e.g., the closed one), the apparent $K_{d\{P\}}$ will be dependent on the fraction of the "active" species as well as its true affinity, such that:

$$K_{d\{P\}}\text{-apparent} = K_{d\{P\}}\text{-true} * (1 + K_{oc}),$$

where K_{oc} = [open]/[closed]. The same $K_{d\{P\}}$-apparent might thus be obtained with a rare, tight-binding form as with a more common, but weaker-binding, form.

Different classes of mutations can be seen to give rise to distinct patterns of effects on measurable experimental properties. The most useful plot for a preliminary analysis would seem to be V_{max} versus a value of $K_{m\{L\}}$ corrected for effects on $K_{d\{L\}}$. Whole cell studies in the related ribose- and arabinose-binding transport systems suggest, for instance, that most of the binding protein mutants that have been isolated are primarily affecting k_4. Mutations of the former protein are much more likely to be accompanied by alterations in $K_{d\{L\}}$ as well, which is consistent with the closer interactions of the two domains in the ligand-bound form in that case. The actual surface of both of these binding proteins that is involved in binding the membrane complex may therefore be larger than has been previously proposed. Mutations outside this region, which were categorized as silent based only on an analysis of V_{max}, may show $K_{d\{PL\}}$ effects on closer analysis. Kehres (1992) pointed out the relationship between V_{max} and $K_{m\{ara\}}$ earlier, also attributing it to a k_4 effect, but because the association of ligand-free binding protein was not considered in that study, the mathematical relationships derived do not appear to be generally applicable. An analysis of two other mutations of the ribose-binding protein sheds new light on other experimental observations.

The obvious goals in modeling studies of this type lie both in the explanation of existing experimental data and in offering new directions for the acquisition of additional information. The parameter sets presented here are viewed as a useful starting point from which future work with both wild-type and mutant proteins can begin. The latter studies seem to provide a means of distinguishing between different models and parameter sets, as well as of suggesting which properties are mostly likely to be affected by any particular mutation.

Materials and methods

The program Mathematica for the Macintosh (Wolfram Research, Champaign, Illinois) was used for most mathematical manipulations and bookkeeping. Derivations and machine-ready versions of the final expressions are found in the Electronic Appendix. Sample scripts and examples of analyses using Mathematica are also available by request from the authors.

Supplementary material in the Electronic Appendix

Subdirectory Shilton.SUP of the SUPLEMNT directory in the Electronic Appendix contains a Microsoft Word file explaining the derivations for Models 1, 2, and 3. Also provided is a text-only file that can be read directly into Mathematica. It contains general expressions for Models 1, 2, and 3: [PLM], [M], v, $K_{m\{L\}}$, $K_{m\{Ptot\}}$.

Acknowledgments

This work was supported by a grant from the Swedish Natural Science Research Council (NFR) to S.L.M. (K-KU 9991-304) and by a postdoctoral fellowship from the Canadian Medical Research Council to B.H.S. We thank Prof. Winfried Boos for several helpful discussions and for sharing information prior to publication.

References

Ames GFL. 1986. Bacterial periplasmic transport systems: Structure, mechanism, and evolution. *Annu Rev Biochem 55*:397–425.

Binnie RA, Zhang H, Mowbray SL, Hermodson MA. 1992. Mutations of the ribose-binding protein of *Escherichia coli* which affect chemotaxis and transport. *Protein Sci 1*:1642–1651.

Björkman AJ, Mowbray SL, Binnie RA, Zhang H, Hermodson MA, Cole LB. 1994. Probing protein–protein interactions: The ribose binding protein of bacterial transport and chemotaxis. *J Biol Chem 269*:20206–20211.

Bohl E, Boos W. 1995. Binding protein-dependent transporters: An answer of mathematics to biology. *J Comput Appl Math*. Forthcoming.

Bohl E, Shuman HA, Boos W. 1995. Mathematical treatment of the kinetics of binding protein-dependent transport systems. *J Theor Biol 172*:83–94.

Boos W, Lucht JM. 1995. Periplasmic binding-protein-dependent ABC transporters. In: Lin E, ed. *Escherichia coli and Salmonella typhimurium: Cellular and molecular biology*. Washington, D.C.: American Society for Microbiology. Forthcoming.

Brass JM, Higgins CF, Foley M, Rugman PA, Birmingham J, Garland PB. 1986. Lateral diffusion of proteins in the periplasm of *Escherichia coli*. *J Bacteriol 165*:787–794.

Davidson AL, Shuman HA, Nikaido H. 1992. Mechanism of maltose transport in *Escherichia coli*: Transmembrane signalling by periplasmic binding proteins. *Proc Natl Acad Sci USA 89*:2360–2364.

Dean DA, Fikes JD, Gehring K, Bassford PJ Jr, Nikaido H. 1989. Active transport of maltose in membrane vesicles obtained from *Escherichia coli* cells producing tethered maltose-binding protein. *J Bacteriol 171*:503–510.

Dean DA, Hor LI, Shuman HA, Nikaido H. 1992. Interaction between maltose-binding protein and the membrane-associated maltose transporter complex in *Escherichia coli*. *Mol Microbiol 6*:2033–2040.

Flocco MM, Mowbray SL. 1994. The 1.9 Å X-ray structure of a closed unliganded form of the periplasmic glucose/galactose receptor from *Salmonella typhimurium*. *J Biol Chem 269*:8931–8936.

Hor LI, Shuman HA. 1993. Genetic analysis of periplasmic binding protein dependent transport in *E. coli*: Each lobe of maltose-binding protein interacts with a different subunit of the $MalFGK_2$ membrane transport complex. *J Mol Biol 233*:659–670.

Jacobson BL, He JJ, Vermersch PS, Lemon DD, Quiocho FA. 1991. Engineered interdomain disulfide in the periplasmic receptor for sulfate transport reduces flexibility. *J Biol Chem 266*:5220–5225.

Kehres DG. 1992. A kinetic model for binding protein-mediated arabinose transport. *Protein Sci 1*:1661–1665.

Kehres DG, Hogg RW. 1992. *Escherichia coli* K12 arabinose-binding protein mutants with altered transport kinetics. *Protein Sci 1*:1652–1660.

Maddock JR, Shapiro L. 1993. Polar location of the chemoreceptor complex in the *Escherichia coli* cell. *Science 259*:1717–1723.

Manson MD, Boos W, Bassford PJ Jr, Rasmussen BA. 1985. Dependence of maltose transport and chemotaxis on the amount of maltose-binding protein. *J Biol Chem 260*:9727–9733.

Miller DM III, Olson JS, Pflugrath JW, Quiocho FA. 1983. Rates of ligand binding to periplasmic proteins involved in bacterial transport and chemotaxis. *J Biol Chem 258*:13665–13672.

Mowbray SL. 1992. The ribose and glucose/galactose receptors: Competitors in bacterial chemotaxis. *J Mol Biol 227*:418–440.

Olah GA, Trakhanov S, Trewhella J, Quiocho FA. 1993. Leucine/isoleucine/valine binding protein contracts upon binding of ligand. *J Biol Chem 269*:16241–16247.

Oliver DB. 1987. Periplasm and protein secretion. In: Neidhardt FC, Ingraham JL, Low KB, Magasanick B, Schaechter M, Umbarger HE, eds. *Escherichia coli and Salmonella typhimurium: Cellular and molecular biology*. Washington, D.C.: American Society for Microbiology. pp 56–69.

Prossnitz E, Gee A, Ames GFL. 1989. Reconstitution of the histidine periplasmic transport system in membrane vesicles. Energy coupling and interaction between the binding protein and the membrane complex. *J Biol Chem 264*:5006–5014.

Richarme G, Kepes A. 1983. Study of binding protein–ligand interaction by

ammonium sulfate-assisted adsorption on cellulose ester filters. *Biochim Biophys Acta 742*:16–24.

Schwartz M, Kellerman O, Szmelcman S, Hazelbauer GL. 1976. Further studies on the binding of maltose to the maltose-binding protein of *Escherichia coli*. *Eur J Biochem 71*:167–170.

Shuman HA. 1982. Active transport of maltose in *Escherichia coli* K-12: Role of the periplasmic maltose binding protein and evidence for a substrate recognition site in the cytoplasmic membrane. *J Biol Chem 257*:5455–5461.

Szmelcman S, Schwartz M, Silhavy TJ, Boos W. 1976. Maltose transport in *Escherichia coli* K12: A comparison of transport kinetics in wild-type and λ-resistant mutants with the dissociation constants of the maltose-binding protein as measured by fluorescence quenching. *Eur J Biochem 65*:13–19.

Treptow NA, Shuman HA. 1985. Genetic evidence for substrate and periplasmic-binding-protein recognition by the MalF and MalG proteins, cytoplasmic membrane components of the *Escherichia coli* maltose transport system. *J Bacteriol 163*:654–660.

van Wielink JE, Duine JA. 1990. How big is the periplasmic space? *Trends Biochem Sci 15*:136–137.

Walsh C. 1979. *Enzymatic reaction mechanisms*. New York: W.H. Freeman.

Wiegel FW. 1983. Diffusion and the physics of chemoreception. *Phys Rep 95*:283–319.

Wolf A, Shaw SW, Nikaido K, Ames GFL. 1994. The histidine-binding protein undergoes conformational changes in the absence of ligand as analyzed with conformation-specific monoclonal antibodies. *J Biol Chem 269*:23051–23058.